Convergence of Cross Sections to Their Peripheral (Born) Limit

Xiaochuan Pan

Department of Physics and James Franck Institute, The University of Chicago, Chicago, Illinois 60637

The electron-ion complex formed in a collision is treated by eigenchannel R-matrix and multichannel quantum-defect methods. Convergence of the results to the limit of peripheral collisions where the Born approximation holds is displayed. Cascade effects are included quantitatively. Extensive results of electron collisions with alkaline-earth ions are illustrated here by the prototype $e + Mg^+$.

Different treatments are appropriate to collisions with large and small impact parameters. Projectile and target remain distinct in *peripheral* (or *grazing*) collisions but form a joint collision complex when their structures intermingle. An earlier paper has indicated how to combine treatments appropriate to large- and short-range collisions.[1] Contributions of the two types to a specific experiment have also been sorted out.[2] We deal specifically with electron-ion collisions but the transition from complex-forming to peripheral processes occurs similarly in nuclear and particle collisions.[3,4] In the example of nuclear scattering two types of peripheral mechanisms may occur, the "Coulomb interaction" outside the barrier and the long-range meson exchange within 1–2 fm; the "nonlocal quark interaction" within a fraction of 1 fm implies a complex formation and is more difficult to treat than in atomic collisions. The question addressed here is how to demonstrate the boundary between complex-forming and peripheral collisions.

Peripheral treatments can be applied to low partial waves readily, regardless of their becoming grossly unrealistic. Treatments of complex-forming collisions can extend to higher partial waves thus becoming increasingly laborious. We compare here results of both treatments proceeding from low to higher partial waves. Their convergence in Fig. 1 will show graphically at what point an additional treatment of the collision complex has become superfluous. This graphical approach appears equally applicable in other fields; a suitable plot of experimental data might replace the calculation of complex-forming collisions in the absence of adequate theory.[2–4]

Calculations of atomic and molecular systems have progressed steadily and laboriously in past decades. A combination of R-matrix and multichannel quantum-defect (MQDT) procedures has recently proved more efficient and more accurate for the study of atomic spectra.[5–9] The same combination is extended here to collisions for the first time and reveals extensive details of the complex formation.

We have chosen the low-energy ($\varepsilon_i \lesssim 13$ eV) electron-ion collision for this study, where major correlations between projectile and target electrons occur and a temporary collision complex is formed.

ε_i (a.u.)
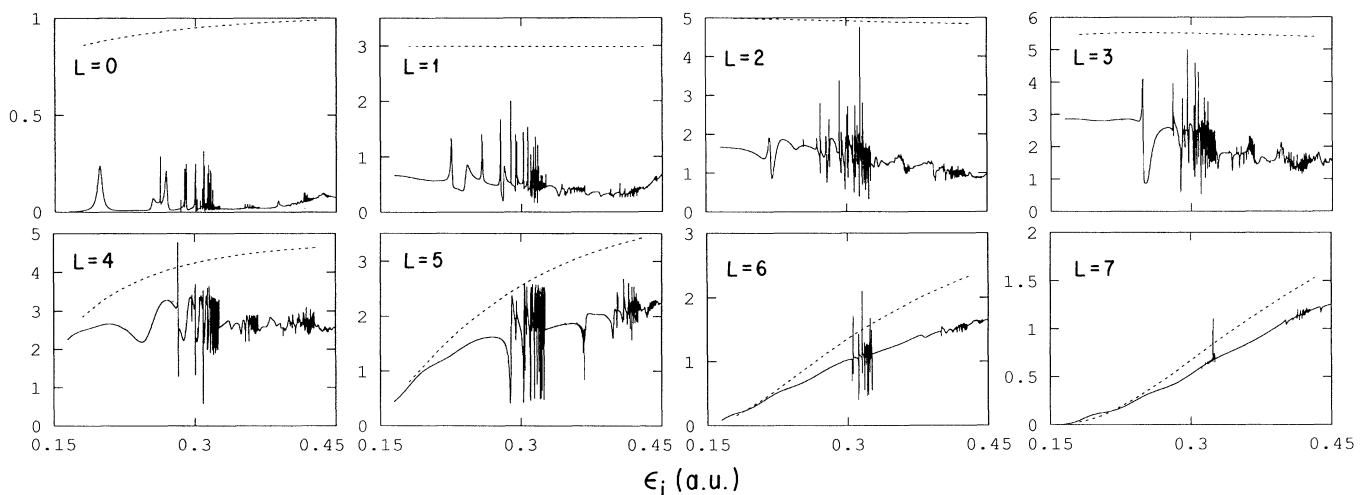
FIG. 1. Dimensionless Coulomb-Born collision strengths $\Omega_{CB}^{L\pi}$ (dashed lines) and $\frac{1}{2}\sum_S \Omega^{LS\pi}$ (solid lines) from the R matrix with MQDT for $Mg^+(3s \to 3p)$. Note the discrepancies at low L and the convergence of $\Omega_{CB}^{L\pi}$ to $\frac{1}{2}\sum_S \Omega^{LS\pi}$ at $L=7$. The abscissa is the incident energy in a.u. here and in the following figures.

This combination allows a systematic treatment of the prominent series of double-excitation states of the complex, which afford valuable and rich structure information about the complex, and applies as well to other processes such as dielectronic recombination. Although fragmentary evidence of such double-excitation series had emerged in earlier experiments[10,11] and calculations,[12-14] application of MQDT is particularly apt to bring out their extensive details.

To evaluate a collision cross section requires, in principle, an infinite number of partial waves. However, no elaborate treatment is needed for the contributions from high partial waves (here $L > 7$) for which the projectile remains peripheral, failing to correlate with target electrons. These contributions may be provided adequately by a Born approximation. The main goal of this paper is to display the convergence of R-matrix results to those of the Coulomb-Born approximation.

Electron collisions with monovalent ions (Be^+, Mg^+, Ca^+) have been chosen for this study as the counterpart to the two-electron spectroscopy of alkaline-earth ions.[8] This paper deals only with the electron-impact excitation of Mg^+, with emphasis on the first optical resonance transition in the target ion $Mg^+(3s \to 3p)$.

The R-matrix method, discussed in detail elsewhere,[8] determines the wave function ψ_β variationally on the surface of a reaction volume V. The ψ_β are eigenstates of the Hamiltonian at any desired energy with a constant normal logarithmic derivative b_β over the surface S that encloses V. Outside this volume, the field is Coulombic and the escaping electronic wave function can be represented as a superposition of regular and irregular energy-normalized Coulomb wave functions f and g by projecting ψ_β onto alternative states ϕ_i of the residual ion on S:[8]

$$\langle \phi_i | \psi_\beta \rangle_S = f_i(r_0) I_{i\beta} - g_i(r_0) J_{i\beta}, \tag{1}$$

$$-b_\beta \langle \phi_i | \psi_\beta \rangle_S = f_i'(r_0) I_{i\beta} - g_i'(r_0) J_{i\beta}, \tag{2}$$

where $i = 1, 2, \ldots, N$. Here N is the number of open or weakly closed channels external to S, and ϕ_i includes the spin and orbital couplings of the escaping electron. The matrix elements $I_{i\beta}$ and $J_{i\beta}$ are determined by Eqs. (1) and (2) and form the $N \times N$ reaction matrix[8]

$$\mathbf{K} = \mathbf{J}\mathbf{I}^{-1}, \tag{3}$$

with diagonalized form

$$K_{ij} = \sum_\alpha U_{i\alpha} \tan(\pi\mu_\alpha) U_{j\alpha}. \tag{4}$$

Numerical diagonalization of Eq. (3) provides the MQDT parameters $\{U_{i\alpha}, \tan\mu_\alpha\}$, namely, the eigenvectors and eigenvalues of the $\mathbf{K}$ matrix which generally depend smoothly on the energy and serve also to predict observables such as the photoionization cross section.[7,8]

The scattering matrix $\mathbf{S}$ and the transition matrix $\mathbf{T}$
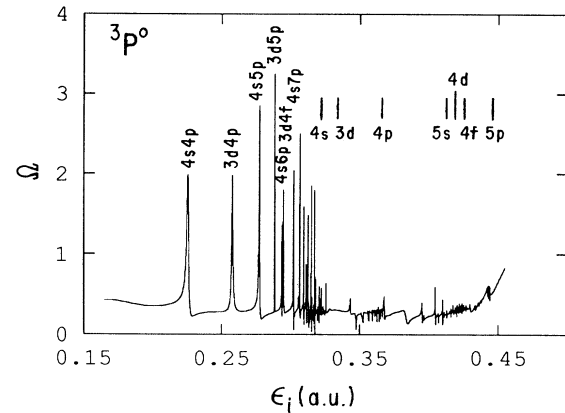
FIG. 2. Dimensionless collision strengths $\Omega^{LS\pi}$ for $Mg^+(3s \to 3p\ ^3P^\circ)$. The small vertical lines in the figures indicate the excitation thresholds of Mg^+.

are evaluated as[4]

$$\mathbf{S} = \frac{1 + i\mathbf{K}^0}{1 - i\mathbf{K}^0}, \quad \mathbf{T} = 1 - \mathbf{S}, \tag{5}$$

where $\mathbf{K}^0$, according to MQDT, is the open-channel portion of the original $\mathbf{K}$, obtained by eliminating all the closed channels as in Eq. (6.29) of Ref. 6. This elimination is equivalent to summing over the effects of an infinite number of discrete states in the closed channels.

The total inelastic cross section for an unpolarized collision results by averaging over initial and summing over final magnetic states of the angular and spin angular momenta and by integrating over angles[6] (in a.u.):

$$\sigma(i \to f) = \frac{\pi}{k_i^2} \sum_{LS\pi} \frac{\Omega^{LS\pi}(i \to f)}{(2S_i + 1)(2L_i + 1)}. \tag{6}$$

The dimensionless collision strength, for each set of total angular momenta and parity $(LS\pi)$, is

$$\Omega^{LS\pi}(i \to f) = \sum_{l_i, l_f} \frac{1}{2}(2L + 1)(2S + 1)|T_{l_i l_f}^{LS\pi}|^2, \tag{7}$$

with the summation extending over the projectile's orbitals.

The LS-coupling scheme is adopted in our R-matrix calculation. The energy range to be treated and the channels $(nl, \varepsilon l')$ retained in the R-matrix calculation dictate the radius of the reaction volume. We have utilized a radius of $r_0 = 31$ a.u., beyond which the wave function is negligible for all (nl) target states of present interest. The number of $(nl, \varepsilon l')$ channels included in the calculation ranged from 13 to 20. Thereby each $\mathbf{I}$ or $\mathbf{J}$ matrix, for each set $(LS\pi)$ and each incident energy, consists of 170 to 400 elements.

Double excitations of the electron-target complex result by transient capture of the projectile electron within an excited target ion. These resonances form prominent infinite series, converging to the excitation thresholds of

TABLE I. Double excitation energies (in eV) [above the ground state $Mg(3s^2)$].

States $^1P^\circ$	Expt.[a]	Present work
$4s4p$	14.18	14.17
$4s5p$	15.24	15.23
$4s6p$	15.61	15.61
$4s7p$	15.83	15.83
$4s8p$	15.98	15.99
$4s9p$	16.06	16.07
$4s10p$	16.11	16.10

[a]References 15 and 16.

Mg^+, in plots of the collision strength $\Omega^{LS\pi}(i \to f)$ for each set of $(LS\pi)$. They lie at series of zeros of the MQDT determinant $|U^c_{ia}(\varepsilon)\sin[\beta_i(\varepsilon) + \pi\mu^c_a(\varepsilon)]| = 0$, with $\{U^c_{ia}, \beta_i, \mu^c_a\}$ from Ref. 7. Figure 2 shows the collision strength for $Mg^+(3s \to 3p\ ^3P^\circ)$.

Some of the resonance series are identified in Fig. 2. Quantum-defect parameters determine the energies of resonances converging to each threshold for excitation of a target level. Classification of individual resonances is, however, complicated by channel interactions. Table I compares the calculated and observed levels of $ns\varepsilon p$ resonances in Mg.

In Fig. 3 curve a compares the total cross section for $Mg^+(3s \to 3p)$ by summing the collision strengths in Eq. (6) up to $L = 7$ with the experimental fluorescence cross section.[10] This cross section falls below the experimental results with increasing energy, but matching of experimental data is achieved by adding contributions from partial waves with $L > 7$ and from optical cascades from higher levels, included in curve c.

Higher partial waves $(L > 7)$ contribute substantially to optical excitations of target ions because of the slow convergence of the dipole interactions. The Coulomb-Born approximation[17] was utilized to calculate the reaction matrix K^0 for $L > 7$ and hence the collision strengths Ω. Figure 1 compares $\Omega^{L\pi}_{CB}$ and $\frac{1}{2}\sum_S \Omega^{LS\pi}$ for $L \leq 7$. The convergence of $\Omega^{L\pi}_{CB}$ to values generated by the R matrix with MQDT at $L = 7$ guarantees that the contributions from $L > 7$ are provided adequately by Coulomb-Born values. We have evaluated $\Omega^{L\pi}_{CB}$ for L from 8 to 20; a cross section including these high partial-wave contributions is shown as curve b in Fig. 3.

The calculated R matrices of each set $(LS\pi)$ contain cross-section information for *all transitions* between target states accessible in our energy range. We have extracted such cross sections readily for several optically forbidden and allowed excitations of the targets, specifically, $\sigma(3s \to 3d)$, $\sigma(3s \to 4s)$, and $\sigma(3s \to 4p)$, all of which contribute to the resonance emission by cascade. Curve c in Fig. 3 is the corresponding emission cross section after inclusion of the cascade effects and of the high partial waves.

Angular distributions of the scattered electrons, par-
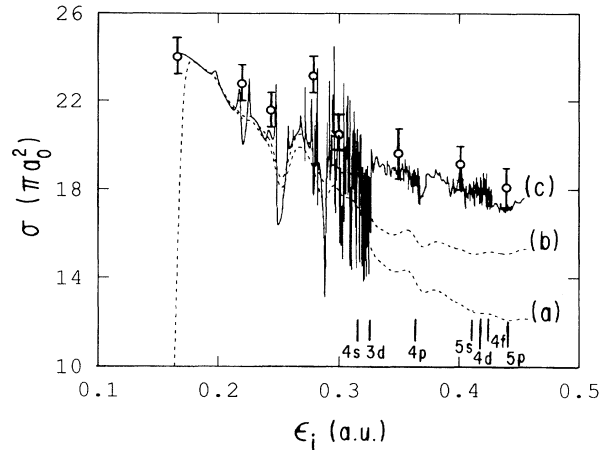
FIG. 3. Total photoemission cross section of $Mg^+(3p \to 3s)$ in πa_0^2. Dashed lines are, curve a, results from the R matrix and MQDT only; curve b, results including high partial waves $(L > 7)$ averaged over a Gaussian of width 0.15 eV, to smooth out most of the resonance structures so that the figure appears uncluttered; solid line, curve c, includes both high partial waves and cascade effects without Gaussian average and displays the detailed resonances; open circles, experiments of Ref. 10.

ticularly interesting near double-excitation resonances, and polarizations of photons emitted by the excited target, in good agreement with experimental results, will be presented elsewhere.

The present work has shown (a) the successful description of a complicated $e + ion$ complex by a combination of the eigenchannel R matrix with MQDT and (b) its quantitative convergence to the peripheral (*Born*) limit. This approach not only gives good agreement with theoretical and experimental cross sections, but affords rich and detailed information on the structures of the collision complex as well as on other processes such as dielectronic recombination.

[1]X. C. Pan and U. Fano, Phys. Rev. A **39**, 4502 (1989); U. Fano and M. Inokuti, Argonne National Laboratory Report No. ANL-76-80, 1976 (unpublished).
[2]X. C. Pan and A. Chakravorty, Phys. Rev. A **41**, 5962 (1990).
[3]R. Machleidt *et al.*, Phys. Rep. **149**, 1 (1987).
[4]T.-S. H. Lee, Phys. Rev. Lett. **50**, 1571 (1983).
[5]U. Fano and C. M. Lee, Phys. Rev. Lett. **31**, 1573 (1973).

[6]M. J. Seaton, Rep. Prog. Phys. **46**, 97 (1983).

[7]C. M. Lee and K. T. Lu, Phys. Rev. A **8**, 1241 (1973).

[8]C. H. Greene and L. Kim, Phys. Rev. A **36**, 2706 (1987).

[9]C. H. Greene, Phys. Rev. A **42**, 1405 (1990).

[10]I. P. Zapesochny et al., Zh. Eksp. Teor. Fiz. **69**, 1948 (1975) [Sov. Phys. JETP **42**, 989 (1976)].

[11]P. O. Taylor, R. A. Phaneuf, and G. H. Dunn. Phys. Rev. A **22**, 453 (1980).

[12]C. Mendoza, J. Phys. B **14**, 2465 (1981).

[13]V. I. Lengyel et al., J. Phys. B **23**, 2847 (1990).

[14]J. Mitroy, D. C. Griffin, and D. W. Norcross, Phys. Rev. A **38**, 3339 (1988).

[15]G. Mehlman-Ballofet et al., Astrophys. J. **157**, 945 (1969).

[16]M. A. Baig and J. P. Connerade, Proc. Roy. Soc. London A **364**, 353 (1978).

[17]P. G. Burgess et al., Philos. Trans. A **266**, 225 (1970).